Modelling of epithelial tissue impedance measured using three different designs of probe

2003 Physiol. Meas. 24 605

(http://iopscience.iop.org/0967-3334/24/2/369)

INSTITUTE OF PHYSICS PUBLISHING PHYSIOLOGICAL MEASUREMENT

Physiol. Meas. **24** (2003) 605–623 PII: S0967-3334(03)59687-3

Modelling of epithelial tissue impedance measured using three different designs of probe

D M Jones, R H Smallwood, D R Hose, B H Brown and D C Walker

Medical Physics and Engineering, University of Sheffield, Royal Hallamshire Hospital, Glossop Road, Sheffield, S10 2JF, UK

E-mail: d.jones@sheffield.ac.uk

Received 18 February 2003
Published 30 April 2003
Online at stacks.iop.org/PM/24/605

Abstract

Impedance measurement is a promising technique for detecting pre-malignant changes in epithelial tissue. This paper considers how the design of the impedance probe affects the ability to discriminate between tissue types. To do this, finite element models of the electrical properties of squamous and glandular columnar epithelia have been used. The glandular tissue model is described here for the first time. Glandular mucosa is found in many regions of the gastrointestinal tract, such as the stomach and intestine, and has a large effective surface area. Firstly, the electrical properties of a small section of gland, with epithelial cells and supportive tissue, are determined. These properties are then used to build up a three-dimensional model of a whole section of mucosa containing many thousands of glands. Measurements using different types of impedance probe were simulated by applying different boundary conditions to the models. Transepithelial impedance, and tetrapolar measurement with a probe placed on the tissue surface have been modelled. In the latter case, the impedance can be affected by conductive fluid, such as mucus, on the tissue surface. This effect has been investigated, and a new design of probe, which uses a guard electrode to counteract this potential source of variability, is proposed.

Keywords: electrical impedance spectroscopy (EIS), Ussing chamber, tetrapolar, guard electrode, finite element analysis, epithelium, squamous, columnar, glandular, gastric, intestinal, tight junctions, lamina propria

1. Introduction

Electrical impedance spectroscopy (EIS) is a novel technique for characterizing tissue properties. Many tissues show a difference in electrical properties between the normal and malignant states. For example, with the onset of cancer, an increase in both conductivity

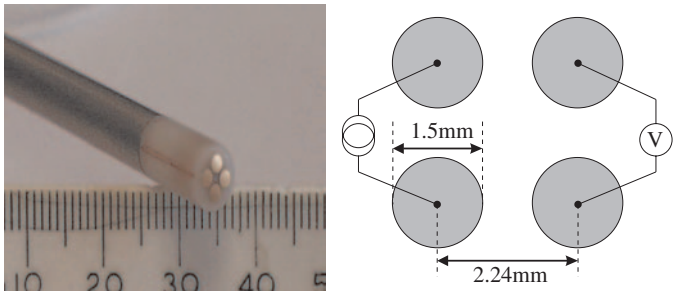

Figure 1. Four-electrode probe used to make measurements on the tissue surface.

and permittivity is seen in breast, liver and muscle tissue (Pethig 1984). We are interested in measurements of epithelial tissue with a view to screening applications—electrical impedance probes offer the potential of rapid, non-invasive diagnosis at minimal cost. Brown *et al* (2000), using the probe shown in figure 1, demonstrated a clear difference between normal and dysplastic cervical epithelium.

The sensitivity and specificity was at least as good as for the Papanicolaou smear test. Gonzalez-Correa *et al* (1999), using a similar probe, were able to differentiate between normal squamous oesophageal tissue and Barrett's oesophagus, a condition in which intestinal columnar epithelium develops at the junction of the stomach and oesophagus. This is associated with a substantially increased risk for adenocarcinoma (Falk 2002).

In the preceding *in vivo* measurements, the current is injected on the surface of the epithelium. This is in contrast to transepithelial measurements, where current is injected *across* the epithelium. The epithelium is mounted in an Ussing chamber, which creates an electrical seal and allows close control of the experimental conditions. The impedance is normalized to the area of exposed epithelium, and so has units of Ω cm^2. This type of measurement is used by electrophysiologists to investigate the ion transportation and barrier properties of epithelia (Barry 1989). Gitter *et al* (1997) describe an Ussing chamber which can perform measurements in the frequency range 1 Hz–65 kHz. The fact that tissue must be clamped in a measurement chamber means that this technique is limited to *ex vivo* samples. It is possible for the tissue adjacent to the clamp to become damaged by crushing, which reduces its impedance. This is a particular problem for small sample chambers (where the fraction of damaged tissue will be high) and for high impedance epithelia.

Computer modelling allows us to investigate how changes in tissue structure affect the impedance spectrum measured with different types of probe. In this way, the probe design can be optimized to detect a particular feature of interest in the tissue. When making measurements using surface probes, it is possible for the tissue to become 'short-circuited' by conductive fluid, such as mucus, on the tissue surface. It is difficult to control the contribution of this component to the measurement and it could lead to variability in the experimental data. For example—fluid may be squeezed out if increased pressure is applied to the probe, thereby reducing the conductance of the short-circuit path. The effect of surface fluid for measurements on an isotropic, homogeneous medium has been investigated by Jones *et al* (2001). For epithelial tissue, the fact that the epithelium acts as a barrier to current flow means that the effects of surface fluid will be accentuated.

Because of this potential source of variability, a new design of probe has been considered. This probe uses a concentrically arranged guard electrode in order to limit the lateral flow of measurement current in the surface fluid.

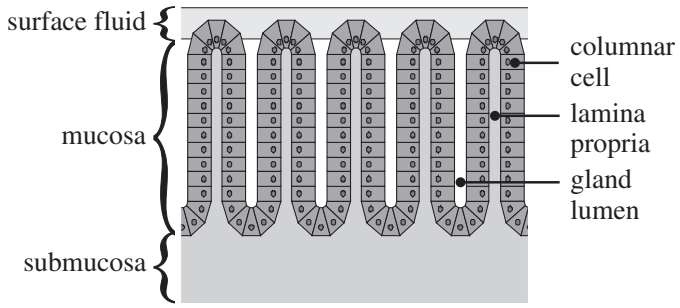

Figure 2. Schematic diagram of a vertical section through glandular mucosa.

In order to test probe designs, finite element models (FEM) of epithelial tissue have been developed. An important characteristic of epithelial tissue is its 'tightness,' which indicates the relative importance of the paracellular and transcellular conduction pathways. In a leaky epithelium, the paracellular current pathway predominates. In a tight epithelium, the paracellular pathway is sealed off by high resistance tight junctions, and the transcellular current pathway is more important (Frömter and Diamond 1972, Powell 1981). The low frequency transepithelial impedance for leaky epithelia is typically much lower than that for tight epithelia.

In this paper, we describe, for the first time, a model of a glandular mucosa which has straight glands. It is possible to change the parameters of the model to give it characteristics of a 'leaky' epithelium, such as that found in the small intestine, or a 'tight' epithelium, such as that found in the body of the stomach. This model has been used to investigate the distinction between abnormal intestinal-type Barrett's oesophageal tissue and the normal gastric-type epithelium of the stomach.

We have also included results for a model of cervical squamous epithelium developed previously by Walker *et al* (2002). This model allows us to investigate the changes occurring with dysplasia, where the epithelium becomes much more leaky than normal.

2. Tissue models

Finite element analysis was used to determine the voltage distribution produced in the tissue when current is applied through external electrodes. This is a numerical technique in which the volume to be modelled is split up into discrete regions of space (elements) whose interactions are mediated through common points (nodes) on the boundaries of the elements. Given the conductivities of the individual elements, a matrix equation can be constructed which relates the nodal voltages ($\mathbf{\Phi}$) to the currents injected at each node ($\mathbf{I}$) through a conductivity matrix ($\mathbf{k}$):

$$\mathbf{k\Phi} = \mathbf{I}.$$

The solution process involves inverting this equation to determine $\mathbf{\Phi}$. A review of finite element analysis applied to bioelectric phenomena is given by Miller and Henriquez (1990).

2.1. Glandular tissue model

Figure 2 shows a schematic diagram of a vertical section through a tissue with straight tubular glands. Figure 3 shows a micrograph of a section parallel to the tissue surface for gastric body

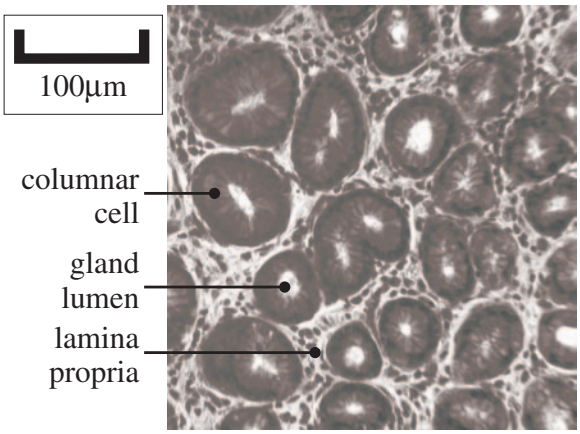

Figure 3. En-face section of gastric mucosa, Masson stain.

mucosa, which has straight glands. The lumen of the glands is surrounded by an epithelium of a single layer of columnar cells. Connective tissue, known as the lamina propria, supports this epithelium and provides a blood supply (Young and Heath 2000, pp 249–73). To cross the mucosa, current flows down the gland lumen (assumed to be filled with conductive fluid), crosses the epithelium and then flows into the lamina propria.

The glandular tissue model is similar in conception to that described by Clausen *et al* (1983). They model a single gland and calculate transepithelial impedance using analytic techniques. The gland is modelled as a transmission line, where the lumen of the gland is connected to the lamina propria at regular intervals by leaky capacitors which represent the epithelial cells. This leads to a distributed impedance and a frequency spectrum with a characteristically broad dispersion.

We have created a FEM with many glands in it, allowing us to extend their idea to model the transverse conduction which occurs when surface tissue probes are used. The analysis is split into two stages. In the first stage, the electrical properties of a section of gland are calculated. In the second stage, the whole mucosa is built up from these gland sections and the boundary conditions for the probe design of interest are applied.

2.1.1. Modelling—stage 1. Figure 4 shows the FEM used for the first part of the analysis. The central section is the lumen of the gland, and this is surrounded by four cells. The lateral intercellular spaces (LIS) are filled with a thin layer of conductive fluid. Around all of the cells, at the edge of the model, is the lamina propria. In figure 4(a), parts of the model have been cut away to allow details of the interior to be seen—one cell has been removed completely, and two of the cells have been opened up to show the cytoplasm and cell membranes. Figure 4(b) shows a sectional view of the model. The connectivity between sections in the FEM is shown in table 1. The cell cytoplasm is joined to other sections of the model via elements modelling a cell membrane with a given conductance and capacitance per unit area. The lateral intercellular space is connected to the gland lumen via a tight junction. The tight junction determines how much current can flow along the paracellular current path. Two types of epithelium have been modelled—a 'perfectly tight' epithelium, in which the tight junction has infinite resistance, and a 'perfectly leaky' epithelium, in which the tight junction has zero resistance. These two extreme cases are used as approximations to gastric- and intestinal-type epithelia, respectively.

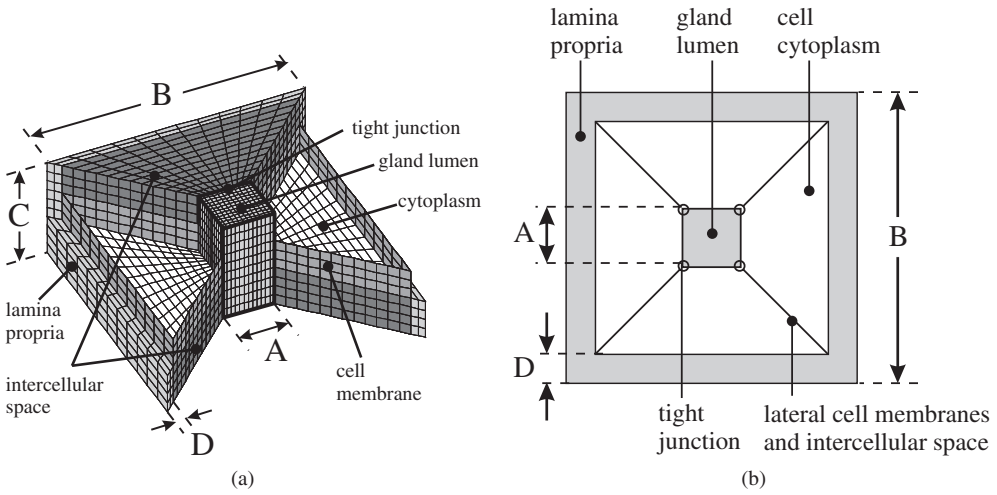

Figure 4. Gland section. Dimensions A to D are given in table 2. (a) 3D cutaway diagram of FEM. (b) Section perpendicular to the gland axis.

Table 1. Connectivity of volume conductors in the model.

Model sections		Linked by
Cell cytoplasm	Lamina propria	Basal cell membrane
Cell cytoplasm	Lateral intercellular space	Lateral cell membrane
Cell cytoplasm	Gland lumen	Apical cell membrane
Lateral intercellular space	Lamina propria	Directly
Lateral intercellular space	Gland lumen	Tight junction (see text)

The properties used in the model are shown in table 2. The cytoplasm conductivity and the cell membrane conductance and capacitance are consistent with the range of values given in a review by Geddes (1972). In addition, the value of cell membrane capacitance divided by conductance (0.01 F Ω for apical, lateral and basal membranes) is of the same order of magnitude as values derived by Clausen *et al* (1983) specifically for gastric mucosa (0.025 F Ω for apical membrane and 0.0035 F Ω for basolateral membrane). For simplicity, the conductivities of all of the volume conductor sections in the model have been given the same value, 1 S m^{-1}. For comparison, Geddes and Baker (1967) give values in the range 0.72 to 1.60 S m^{-1} for animal serum, and values in the range 1.43 to 1.59 S m^{-1} for human plasma (all values at body temperature). The thickness of lateral intercellular space is consistent with the values given by Spring and Hope (1978). Other linear dimensions used in the model are representative of typical values taken from our observations of micrographs of glandular tissue.

The lamina propria provides a low resistance path for current flow. Its dimensions can be changed by inflammation or oedema. The model has been solved with two thicknesses of lamina propria, which lead to either 8% or 15% of the total mucosa volume being occupied by lamina propria.

The electrical properties of the stage 1 FEM of the gland section are characterized by applying four different boundary condition sets, as shown in table 3.

Table 2. Properties used in the stage 1 model.

Property	Value	Unit
Side of gland lumen (A)	10	μm
Side of the whole of the model (B)	50	μm
Height of columnar cells (i.e. dimension along gland lumen) (C)	20	μm
Half-thickness of lamina propria section of model (D)	1 or 2[a]	μm
Thickness of lateral intercellular space	0.5	μm
Conductivity of contents of gland lumen	1	S m^{-1}
Conductivity of cell cytoplasm	1	S m^{-1}
Conductivity of lamina propria	1	S m^{-1}
Conductivity of lateral intercellular space	1	S m^{-1}
Cell membrane capacitance per unit area (apical, basal and lateral)	0.01	F m^{-2}
Cell membrane conductance per unit area (apical, basal and lateral)	1	S m^{-2}

[a] Model solved for two different values of lamina propria half-thickness. A half-thickness of 1 μm gives 8% of the mucosa volume occupied by lamina propria. A half-thickness of 2 μm gives 15% lamina propria.

Table 3. Four boundary conditions applied to the stage 1 model.

Boundary condition	Property
Voltage applied across two opposite sides of the model	Bulk complex conductivity in the transverse direction
Voltage applied across the top and bottom of the model	Bulk complex conductivity in the vertical direction
Voltage applied between gland lumen and the outside of the lamina propria section	Complex conductance per unit length of gland across the epithelial barrier
Voltage applied between the top and bottom of the gland lumen	Conductance vertically along the gland lumen

2.1.2. Modelling—stage 2. The gland section model in stage 1 consists of 13 344 elements and occupies a volume of 50 μm $\times$ 50 μm $\times$ 20 μm $= 5 \times 10^4$ μm^3. To simulate a measurement made using a probe of the size of the order of 1 mm, a tissue volume of at least 10^9 μm^3 must be modelled—a factor 20 000 greater. If the gland section model was simply replicated to cover this volume, then this would produce a model with 267 million elements. It is impractical to solve a model of this size using the currently available computing power. The model of the gland section must be reduced to a single element encapsulating its essential electrical properties. The essential properties are exactly those four described in table 3, obtained by solving the stage 1 model with four different boundary condition sets. The single 'gland section' element which is given these properties has ten nodes (figure 5(c)) and is constructed as follows. It is based on the standard eight node solid hexahedral element used to model conduction in a continuum (figure 5(a)). In general, the conductivity can be anisotropic, with different principal conductivities, 'K_{XX}', 'K_{YY}' and 'K_{ZZ}' being specified along the coordinate axes. 'Z' is taken to be along the direction of the gland. The symmetry in the model indicates that the 'x' and 'y' directions are interchangeable, and so $K_{XX} = K_{YY}$. In order to model conduction along glands, two nodes are added to this element, in the centre of the top and bottom faces. The eight original nodes can be regarded as being in the lamina propria, and the two new nodes are in the gland lumen. This additional compartment to the element is required because it is possible for the gland lumen and adjacent lamina propria to be decoupled electrically from each other so that the electric

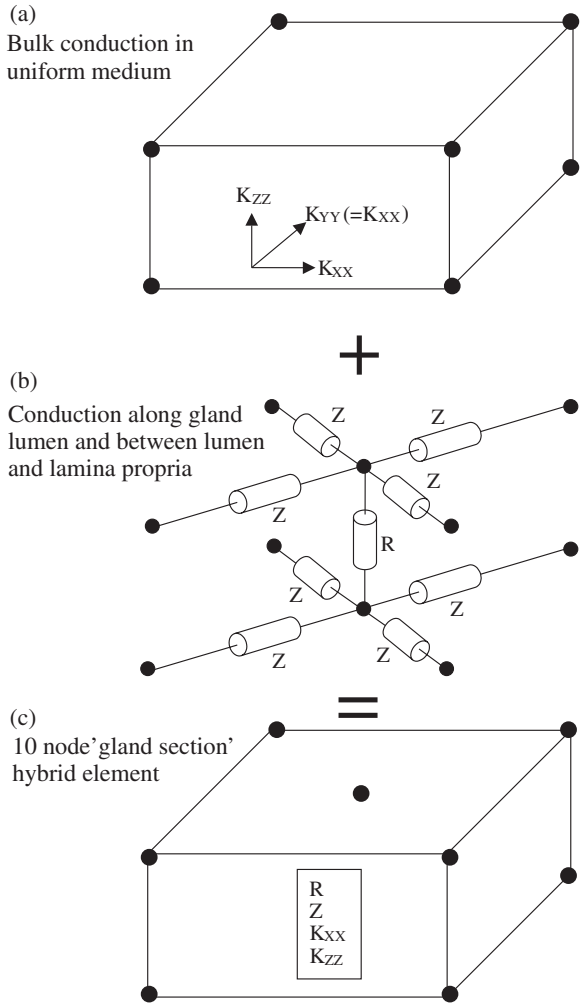

Figure 5. The hybrid 'gland section' element (c) is made up from a section representing conduction in a uniform medium (a) and a section representing conduction between the lamina propria and the gland lumen and conduction along the gland lumen (b).

potential cannot be represented in a single continuum. Figure 5(b) shows the additional conduction pathways introduced into the element. Resistance '*R*' models conduction along the gland lumen, and impedances '*Z*' model conduction between the lumen and the lamina propria.

The values of R, Z, K_{XX} and K_{ZZ} are specified so that the element behaves in the same way as the FEM in stage 1 when subjected to the same four boundary condition sets.

The model for the second stage of analysis is constructed by stacking gland section elements vertically to form complete glands, and then repeating glands horizontally to form a three-dimensional section of mucosa. A conductive mucous layer is added to the surface of the mucosa. Because this layer is thin, two-dimensional 'shell' elements are used. These model transverse conduction across the surface of the mucosa, but have zero impedance in the vertical direction. A thick, uniform layer of submucosa is added to the bottom of the model.

Table 4. Properties used in the stage 2 model.

Layer	Thickness (μm)	Conductivity (S m^{-1})
Mucus	10	1
Mucosa	1000	From stage 1 model
Submucosa	3000	1

The connectivity of the FEM is such that current enters the top of the mucosa only through the gland lumen nodes in the centre of the gland section elements. Conversely, current leaves the bottom of the mucosa only through the lamina propria nodes on the edges of the elements. This ensures that at some point, the current must cross the epithelial cell barrier, represented by impedance '*Z*' in figure 5(b). The properties of the components of the stage 2 model are shown in table 4. The complete glandular tissue models were solved at 36 frequencies in the range 1 Hz–10 MHz.

2.2. Squamous tissue model

This model, developed previously by Walker *et al* (2002), describes the stratified squamous epithelium of the uterine cervix. Briefly, this model comprises several cell layers, each having different electrical properties. In normal tissue, the surface cells are flat and tightly joined together so that there is little intercellular space. The underlying cells are more cuboidal in shape, and there is a greater thickness of intercellular space between cells. In pre-cancerous tissue, the surface cells take on characteristics of the deeper cells, because of lack of normal differentiation. The increased intercellular space for surface cells results in a reduced physiological and electrical barrier. Two models have been considered—normal squamous tissue and severe dysplasia, designated CIN3 (cervical intra-epithelial neoplasia grade 3). The squamous tissue models were solved at nine frequencies in the range 100 Hz–1 MHz.

3. Probe design simulations

3.1. Transepithelial impedance measured with an Ussing chamber

To determine the transepithelial impedance, boundary conditions were applied to the models to simulate electrodes applied to the lumenal and serosal surfaces of the mucosa. For practical measurements, as much submucosal tissue as possible is removed so that it does not contribute to the overall impedance. For this reason, submucosal tissue has not been included in the modelled transepithelial measurement.

3.2. Four-electrode surface probe

The probe shown in figure 1 was used as the design for modelling a tetrapolar measurement. Separate pairs of electrodes are used to drive current and measure voltage—this helps to minimize the effect of electrode impedance. The modelled results show the transfer impedance, which is the measured voltage divided by the injected current. The electrodes have a diameter of 1.5 mm and the centres of adjacent electrodes are separated by 2.24 mm. This probe has been used to make measurements on cervical tissue (Brown *et al* 2000), and a similar probe has been used to make measurements on oesophageal tissue (Gonzalez-Correa *et al* 1999).

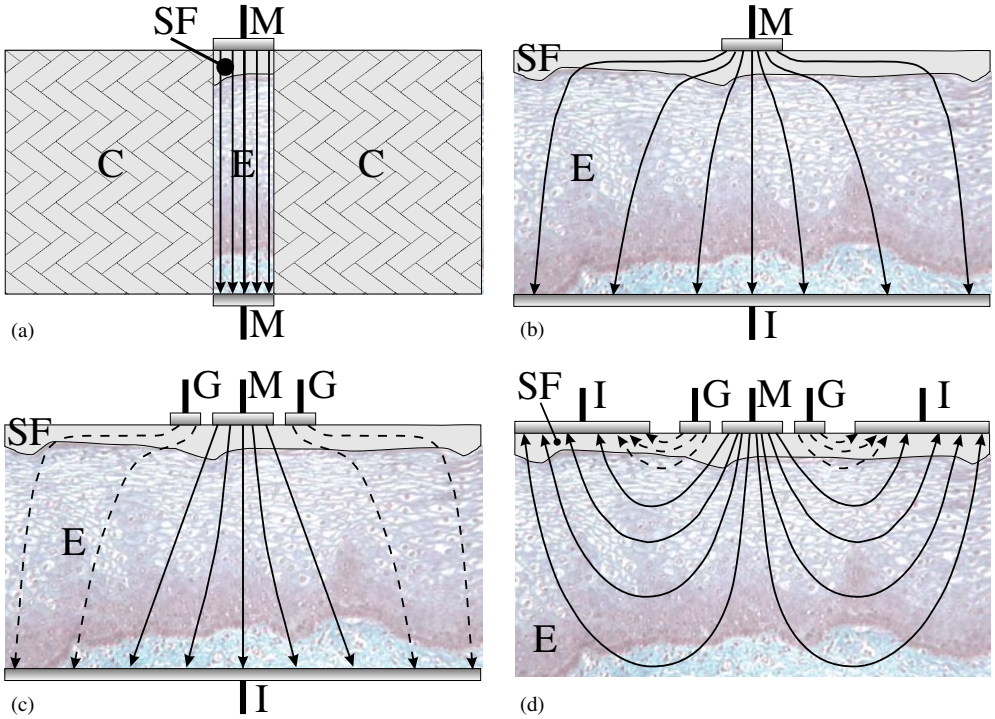

Figure 6. Development of a surface probe to emulate transepithelial impedance measurement. C is a clamp to hold the tissue, E is the epithelium, SF is a layer of surface conductive fluid, M is the measurement electrode, G is an annular guard electrode, I is an indifferent electrode. Solid arrows indicate measurement current flow, dashed arrows represent guard current flow. (a) Transepithelial impedance measurement. (b) Clamp removed and serosal electrode made very large ('indifferent'). (c) Guard electrode added to prevent lateral flow of the measurement current. (d) Indifferent electrode moved from the serosal to the lumenal surface. The drive scheme for the guard electrode is shown in figure 7.

Because this probe makes *in vivo* measurements, submucosal tissue has been included in the models in this case.

3.3. Guarded probe with concentric electrodes

Conceptually, the guarded probe design was developed from the transepithelial measurement configuration. In a transepithelial measurement, the current flow is perpendicular to the surface fluid layer. We wanted to reproduce this situation with a probe which could be placed on the lumenal surface of the epithelium.

Figure 6(a) shows a schematic diagram of a transepithelial measurement, with an electrical seal being made by fixing the epithelium in a clamp ('C' in the figure). In order to make *in vivo* measurements, the clamp must be removed from the tissue (figure 6(b)). Since it is the impedance of the epithelium itself which is of interest, and not the underlying submucosa, the serosal electrode is made into a very large indifferent electrode (I). Any conductive fluid on the tissue surface (SF) will cause the impedance to decrease. This is because the current can spread out laterally, increasing the effective area of the measurement electrode (M).

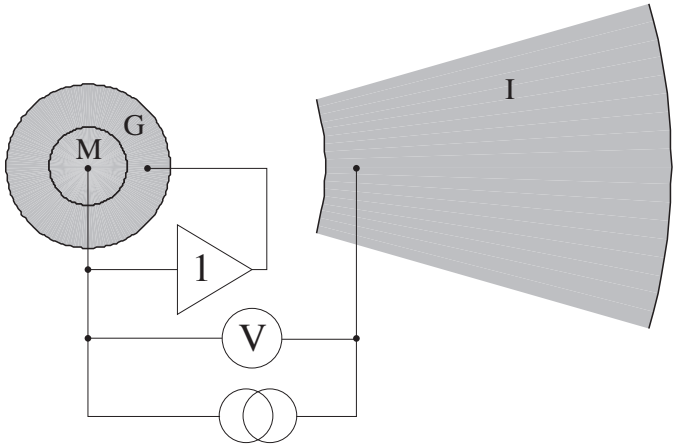

Figure 7. Guarded probe with concentric electrodes. M is the measurement electrode (radius 0–400 μm), G is the guard electrode (radius 400–840 μm) and I is the indifferent electrode (radius 2435–5985 μm).

To prevent this from happening, an annular guard electrode (G) can be placed just outside the measurement electrode (figure 6(c)). The guard electrode is maintained at the same voltage as the measurement electrode. This ensures a well-defined area for current injection by preventing lateral current flow.

The final step is to consider the position of the indifferent electrode (I). It is possible to move this from the serosal surface to the lumenal surface of the epithelium (figure 6(d)). The indifferent electrode is now in the shape of a large annulus surrounding both the measurement and the guard electrodes. There will now be some contribution to the overall impedance from the epithelium underlying the indifferent electrode. However, if the area of the indifferent electrode is much greater than the area of the measurement electrode, most of the contribution to the impedance will arise from the epithelium underneath the measurement electrode.

The electrical connections to the electrodes are shown in figure 7. A feedback loop with a unity gain amplifier maintains the guard electrode at the same voltage as the measurement electrode. The current injected through the measurement electrode is controlled, and this is termed the measurement current. The impedance is calculated as the voltage at the measurement electrode divided by this measurement current. Clearly, current is also injected at the guard electrode, but this does not form part of the measurement current used in the calculation. The purpose of the guard electrode is simply to prevent lateral flow of the measurement current. Figure 7 also shows the dimensions of the electrodes used in the model, with the gap between the guard and measurement electrodes being infinitesimally small.

Boundary conditions were applied to the models to simulate this drive scheme. Submucosal tissue has been included in the models for this measurement.

4. Results

Three pairs of comparisons between epithelial models were made (table 5). The first comparison considers the effect of changing the tight junction resistance in the glandular tissue model. The second comparison considers the effect of lamina propria volume fraction in the glandular tissue model. Finally, normal and CIN3 squamous models are compared.

Table 5. Comparison between three pairs of tissue models. Models can be compared using the impedance at a single frequency, indicated by 'f' in the table.

Tissue	f (Hz)	Comparison	
(a) Glandular columnar	1	Tight gastric 15% lamina propria	Leaky intestinal 15% lamina propria
(b) Glandular columnar	10 000	Leaky intestinal 8% lamina propria	Leaky intestinal 15% lamina propria
(c) Squamous	100	Tight squamous	Leaky CIN3

4.1. Transepithelial impedance measured with an Ussing chamber

The modelled impedance spectra are shown in figure 8. The spectrum for the tight glandular epithelium shown in figure 8(a) has two frequency dispersions. The step size of the low frequency dispersion depends upon the 'tightness' of the epithelium—high resistance tight junctions are needed in order to see a dispersion. For the leaky epithelium model, the low frequency dispersion disappears. The step size of the high frequency dispersion depends upon on the lamina propria volume fraction, as shown by figure 8(b).

For the normal squamous model (figure 8(c)), there is just one dispersion. This dispersion is significantly reduced in size for the leaky CIN3 model.

For both squamous and glandular tissue, the epithelial barrier integrity determines the magnitude of the low frequency impedance. Pre-cancerous (CIN3) tissue presents a much poorer barrier than normal tissue and hence has a lower impedance. Similarly, for glandular tissue, leaky intestinal type epithelium is less of a barrier than tight gastric type epithelium. In squamous tissue, however, the impedance attains its maximum value at a higher frequency—approximately 100 Hz—as compared to glandular tissue, where the impedance reaches its maximum at approximately 1 Hz.

4.2. Four-electrode surface probe

The modelled impedance spectra are shown in figure 9. Comparing these spectra to the corresponding spectra in figure 8, it can be seen that the general form is the same. There are slight differences in shape, the most noticeable being the low frequency dispersion in tight glandular tissue. For the transepithelial measurement (figure 8(a)), there is quite a long tail to this dispersion in the region 10^2–10^4 Hz, but this tail is absent in the four-electrode measurement (figure 9(a)).

Another significant difference is the fact that the four-electrode probe measurement can be affected by conductive surface fluid. The spectra shown are for a surface layer of thickness 10 μm and conductivity 1 S m^{-1}. In order to further investigate the effect of surface fluid, its conductivity was fixed at 1 S m^{-1} and its thickness varied in 13 steps from 0.01 to 100 μm. Note that because the conductive layer is thin, doubling the conductivity will have the same effect as doubling the thickness. In experiments, the conductivity can be decreased by washing the tissue surface with tap water, and this has the same effect as reducing the fluid thickness.

The impedance measured at a particular frequency is plotted against the thickness of surface fluid (figure 10). The frequencies used for the three comparisons are shown in table 5, and the corresponding points in figure 9 have been circled. Comparisons (a) and (c) are between tight and leaky epithelia. In these cases, the lowest modelled frequency (1 Hz for the glandular model, 100 Hz for the squamous model) is used to give the greatest separation.

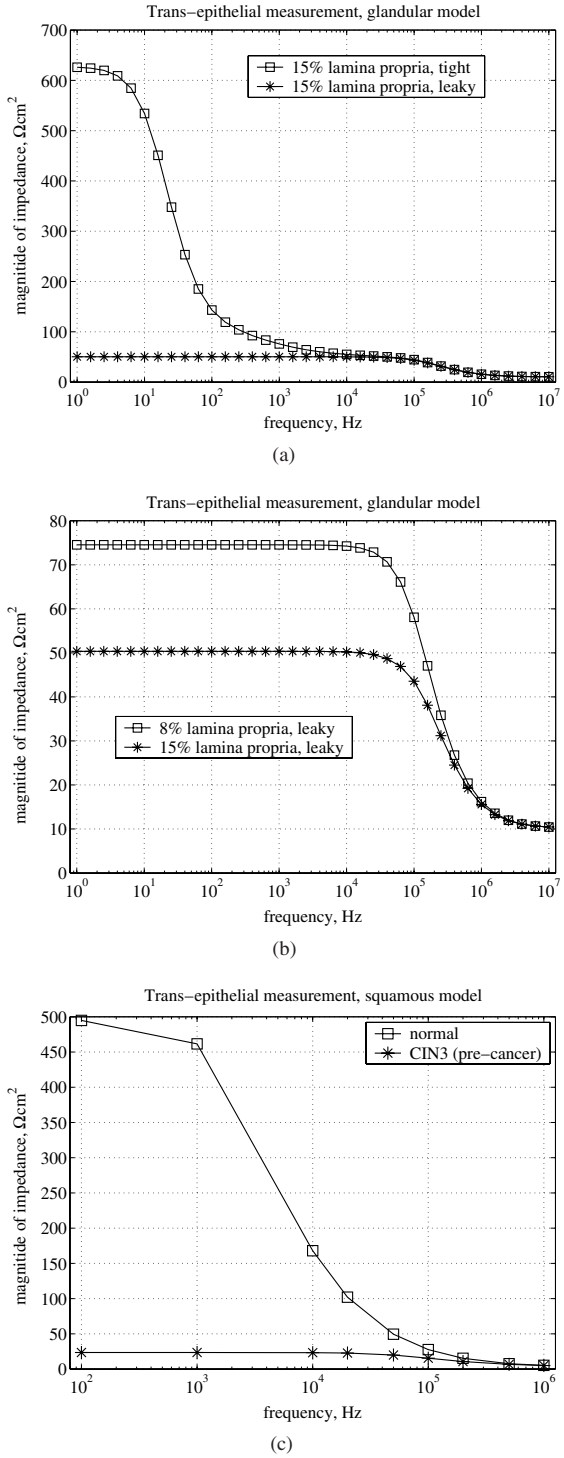

Figure 8. Modelled transepithelial impedance spectra. (a) Glandular tissue, effect of epithelial tightness, (b) glandular tissue, effect of lamina propria volume fraction, (c) squamous tissue, comparison of normal and pre-cancerous (CIN3) states.

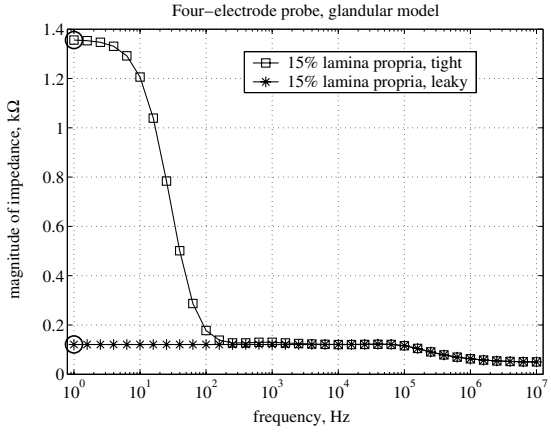

(a)

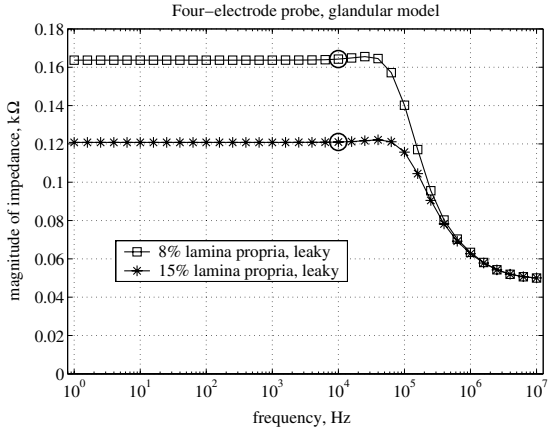

(b)

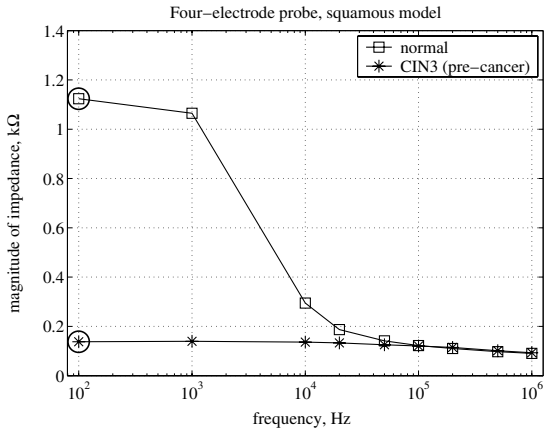

(c)

Figure 9. Modelled spectra for four-electrode probe measurement. (a) Glandular tissue, effect of epithelial tightness, (b) glandular tissue, effect of lamina propria volume fraction, (c) squamous tissue, comparison of normal and pre-cancerous (CIN3) states. Circled points are used to distinguish between tissue types, and correspond to the circled points in figure 10.

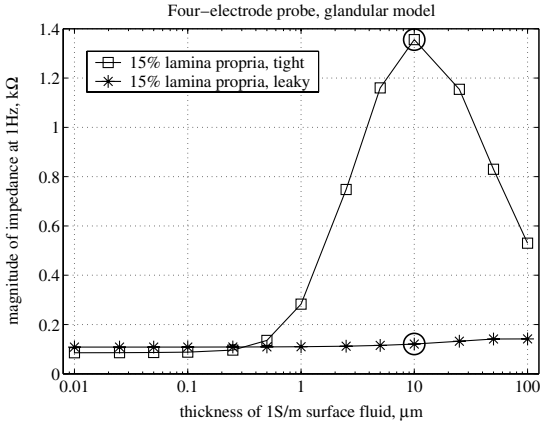

(a)

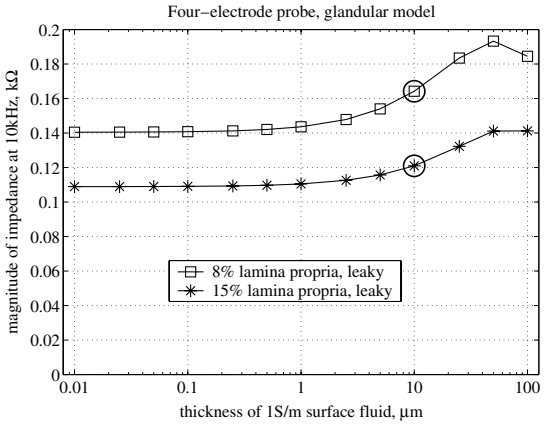

(b)

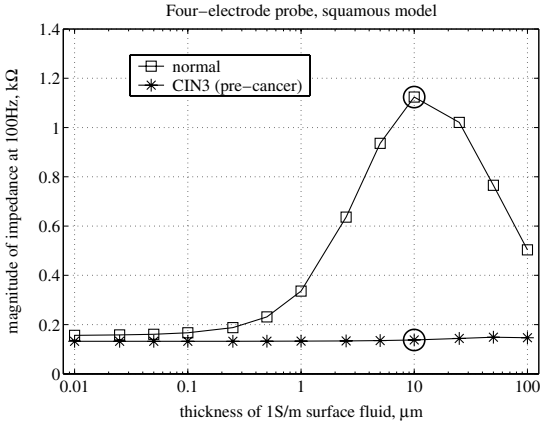

(c)

Figure 10. Modelled effect of conductive surface fluid on the four-electrode probe measurement at a specific frequency. (a) Glandular tissue, effect of epithelial tightness, frequency = 1 Hz, (b) glandular tissue, effect of lamina propria volume fraction, frequency = 10 kHz, (c) squamous tissue, comparison of normal and pre-cancerous (CIN3) states, frequency = 100 Hz. Common points in figures 9 and 10 have been circled.

A frequency of 10 kHz is used to compare glandular tissue models with different lamina propria volume fractions. The impedance at this frequency is unaffected by epithelial tightness.

It can be seen that the surface fluid has a large effect on the impedance of normal squamous tissue at 100 Hz and tight glandular tissue at 1 Hz. It also has an effect, albeit smaller, on the impedances measured for the other models.

4.3. Guarded probe with concentric electrodes

The modelled impedance spectra are shown in figure 11. These graphs are closer in appearance to the transepithelial measurement (figure 8) than the four-electrode measurement (figure 9). In particular, the tight glandular tissue spectrum (figure 11(a)) shows the same long tail between 10^2 and 10^4 Hz for the low frequency dispersion as the transepithelial measurement. The effect of surface fluid was investigated in the same way as for the four-electrode probe measurement, and the results are shown in figure 12. The relationship between the graphs in figures 11 and 12 is indicated by circling the corresponding points.

The graphs show well-separated, almost horizontal lines. This indicates a large distinction between tissue types which is affected little by the surface fluid properties.

5. Discussion

The general shape of the impedance spectra is similar for the three different types of measurement configuration. Slight differences are seen with the four-electrode probe, where the dispersions appear to be narrower. In addition, the four-electrode measurement can be significantly affected by surface fluid, as shown in figure 10.

In both squamous and glandular tissue, the epithelial tightness affects the low frequency impedance measured with all types of probe. However, the structure of squamous and glandular tissue is very different. The squamous model is composed of several layers of cells, whereas the glandular model has only a single cell layer, which is folded to create glands. These differences mean that maximum impedance occurs at a lower frequency for glandular tissue than for squamous tissue. The folded nature of the glandular epithelium means that the supporting lamina propria is present throughout the depth of the mucosa. The lamina propria provides a low resistance current pathway, and the effect of this is seen in a second dispersion at higher frequencies in the impedance spectrum.

For glandular tissue, it is possible that other model parameters will affect the impedance spectrum, e.g., the epithelial depth, gland size and the spacing between glands. In particular, changes to parameters which have the effect of increasing the effective epithelial surface area will make the epithelium appear to be more conductive. In certain glandular epithelia, such as the small intestine, villi are present, but these have not been included in our model. Their effect would be to increase the epithelial surface area, and hence increase the overall conductance of the tissue.

The transepithelial measurement is independent of surface fluid. At low frequency, it distinguishes well between tight and leaky epithelia. For glandular tissue, the impedance at higher frequencies ($\sim$10 kHz) can be used to provide an indication of the lamina propria volume fraction. However, it is not practical to measure transepithelial impedance for *in vivo* clinical diagnosis because access to the serosal surface is required, and the tissue sample must be fixed within a measurement chamber. Non-invasive measurements must be considered.

Tetrapolar surface probes can and have been used to make *in vivo* measurements, but they are affected by surface fluid, and this complicates interpretation of experimental results. Interestingly, it appears that some surface fluid is actually required to see a difference between

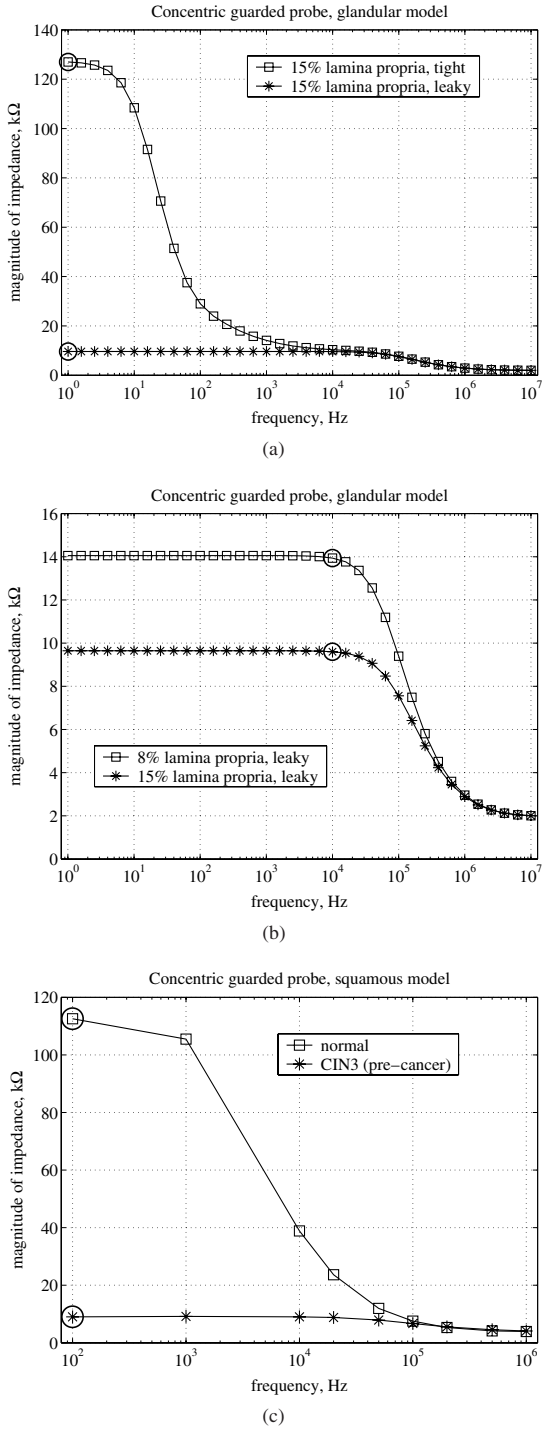

Figure 11. Modelled spectra for concentric guarded probe measurement. (a) Glandular tissue, effect of epithelial tightness, (b) glandular tissue, effect of lamina propria volume fraction, (c) squamous tissue, comparison of normal and pre-cancerous (CIN3) states. Circled points are used to distinguish between tissue types, and correspond to the circled points in figure 12.

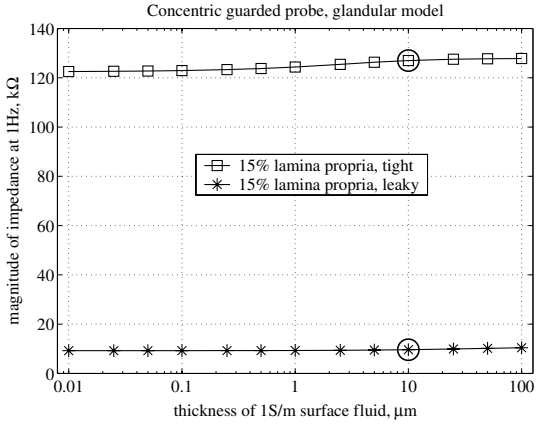

(a)

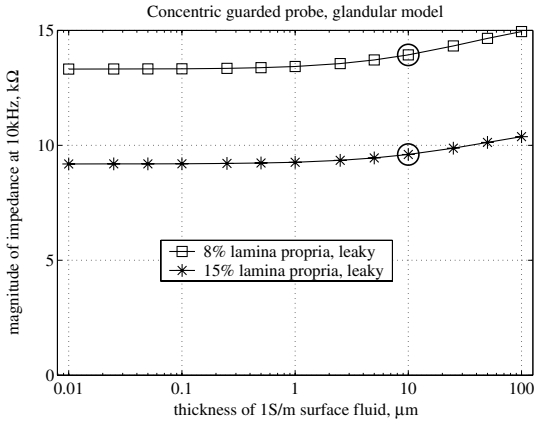

(b)

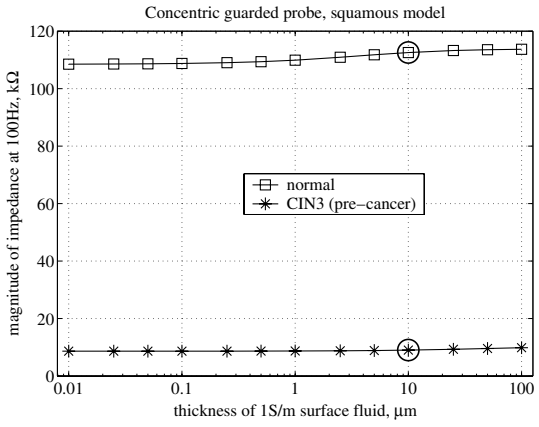

(c)

Figure 12. Modelled effect of conductive surface fluid on the guarded concentric probe measurement at a specific frequency. (a) Glandular tissue, effect of epithelial tightness, frequency = 1 Hz, (b) glandular tissue, effect of lamina propria volume fraction, frequency = 10 kHz, (c) squamous tissue, comparison of normal and pre-cancerous (CIN3) states, frequency = 100 Hz. Common points in figures 11 and 12 have been circled.

the tight and leaky epithelia—if the surface fluid thickness is reduced to zero, then the distinction between the two types becomes very small (figures 10(a) and (c)). For low values of surface fluid thickness, the slope of the graphs in this figure is positive. This corresponds to a negative sensitivity for the transfer impedance, i.e. increasing the conductance of the surface path increases the transfer impedance. For high values of surface fluid thickness, the slope of the graphs becomes negative, corresponding to a positive sensitivity.

Although the tetrapolar impedance is generally higher in a tight epithelium than in a leaky epithelium, the amount by which the impedance is higher is strongly dependent on the surface fluid properties. This makes it impossible to make quantitative predictions about the tightness of epithelia with intermediate properties from a four-electrode surface probe measurement. An average of many readings may show differences between tissue types, but there will be a significant amount of scatter on individual data points. Similarly, although an increase in the lamina propria volume fraction will, on average, decrease the impedance at 10 kHz (figure 10(b)), individual readings may be affected by variations in surface fluid properties. Experimental impedance measurements suggest that for unwashed tissue samples, the surface fluid thickness is somewhere in the region of 10 to 100 μm.

Ideally, we would like the plots of impedance versus surface fluid thickness to show horizontal lines, with a consistent, large separation between different tissue classifications. The results for the guarded concentric probe (figure 12) are very encouraging from this point of view, with large separations between the different pairs of tissue types. This shows that in principle, the guarding scheme is effective in preventing the surface fluid from affecting the results.

However, the practicalities of probe measurement must also be considered. Because the guarded probe makes a bipolar measurement, the electrode impedance contributes to the measurement, and this must be minimized as far as possible. This is especially important given that electrode impedance can become very large at the low frequencies required to investigate epithelial barrier integrity. The electrode impedance could become much greater than the tissue impedance, and it could also prevent the guarding mechanism from functioning effectively. There are several techniques for reducing the impedance of an electrode by treating it to increase its effective surface area. One example is the platinization process for platinum electrodes (Geddes 1972) which can decrease the electrode impedance by a factor of 100 to 1000. More recently, Hubmann *et al* (1992) have investigated treatments which involve sputtering the electrode surface with either titanium nitride or iridium. This results in a fractal surface which has a very high effective surface area.

For practical probe designs, a finite space between the measurement and guard electrodes is required for insulation purposes. Computer modelling has shown that a large gap can reduce the efficacy of the guarding process, and so the separation should be kept as small as possible.

6. Conclusions

A new FEM of the electrical properties of glandular mucosa has been constructed. A previously described model of squamous tissue was also used. These models allow us to determine how the impedance spectrum is affected by changes in the tissue structure. In particular, the tightness of the epithelium affects the low frequency impedance. In the glandular model, the properties of the lamina propria affect the impedance at intermediate frequencies ($\sim$10 kHz). Measurements using Ussing chambers and tetrapolar surface probes have been simulated. The tetrapolar surface probe measurements were found to be highly influenced by the presence of even a thin layer of conductive fluid on the tissue surface. To counteract this effect, a new

design of probe, which uses a concentric guard electrode, has been considered. Modelling has shown this design to be very effective at making measurements which are independent of the surface fluid properties. However, in order to make practical measurements, the effect of electrode impedance would need to be taken into account.

Acknowledgments

The authors would like to thank Dr K D Bardhan, Dr T J Stephenson, Mr C J Stoddard and Dr C A Gonzalez-Correa for their invaluable assistance.

References

Barry P H 1989 Ionic permeation mechanisms in epithelia: biionic potentials, dilution potentials, conductances, and streaming potentials *Methods Enzymol.* **171** 678–715

Brown B H, Tidy J A, Boston K, Blackett A D, Smallwood R H and Sharp F 2000 Relation between tissue structure and imposed electrical current flow in cervical neoplasia *Lancet* **355** 892–95

Clausen C, Machen T E and Diamond J M 1983 Use of AC impedance analysis techniques to study membrane changes related to acid secretion in amphibian gastric mucosa *Biophys. J.* **41** 167–78

Falk G W 2002 Barrett's esophagus *Gastroenterology* **122** 1569–91

Frömter E and Diamond J 1972 Route of passive ion permeation in epithelia *Nature New Biol.* **235** 9–13

Geddes L A 1972 *Electrodes and the Measurement of Bioelectric Events* (New York: Wiley)

Geddes L A and Baker L E 1967 The specific resistance of biological material—a compendium of data for the biomedical engineer and physiologist *Med. Biol. Eng.* **5** 271–93

Gitter A H, Schulzke J D, Sorgenfrei D and Fromm M 1997 Using chamber for high-frequency transmural impedance analysis of epithelial tissues *J. Biochem. Biophys. Methods* **35** 81–8

Gonzalez-Correa C A, Brown B H, Smallwood R H, Kalia N, Stoddard C J, Stephenson T J, Haggie S J, Slater D N and Bardhan K D 1999 Virtual biopsies in Barrett's esophagus using an impedance probe *Ann. NY Acad. Sci.* **873** 313–21

Hubmann M, Hardt R, Bolz A and Schaldach M 1992 Long-term performance of stimulation and sensing behaviour of TiN and Ir coated pacemaker leads having a fractal surface structure *Proc. 14th Ann. Int. Conf. IEEE (Paris)* pp 2379–80

Jones D M, Smallwood R H, Hose D R and Brown B H 2001 Constraints on tetrapolar tissue impedance measurements *Electron. Lett.* **37** 1515–7

Miller C E and Henriquez C S 1990 Finite element analysis of bioelectric phenomena *Crit. Rev. Biomed. Eng.* **18** 207–33

Pethig R 1984 Dielectric properties of biological materials: biophysical and medical applications *IEEE Trans. Electr. Insulat.* **19** 453–74

Powell D W 1981 Barrier function of epithelia *Am. J. Physiol.* **241** G275–88

Spring K R and Hope A 1978 Size and shape of the lateral intercellular spaces in a living epithelium *Science* **200** 54–8

Walker D C, Brown B H, Smallwood R H, Hose D R and Jones D M 2002 Modelled current distribution in cervical squamous tissue *Physiol. Meas.* **23** 159–68

Young B and Heath J W 2000 *Wheater's Functional Histology* (London: Harcourt)